

⁸Lin, C. C., *Turbulent Flows and Heat Transfer*, 1959.

⁹Van Driest, E. R., "Turbulent Boundary Layer in Compressible Flows," *Journal of Aeronautical Sciences*, Vol. 18, No. 3, 1951, p. 145.

¹⁰Ozcan, O., and Holt, M., "Supersonic Separated Flow Past a Cylindrical Obstacle on a Flat Plate," *AIAA Journal*, Vol. 22, No. 5, 1984, pp. 611-617.

Solution-Adaptive Approach for Unsteady Flow Calculations on Quadrilateral-Triangular Meshes

C. J. Hwang* and J. M. Fang†
National Cheng Kung University,
Tainan, Taiwan, Republic of China

Introduction

IN recent years, considerable effort has been made in the development of solution-adaptive methods for solving the unsteady Euler equations on unstructured meshes. Several impressive approaches,¹⁻³ which include the numerical schemes and adaptive mesh techniques, were presented to efficiently obtain higher spatial accuracy in the flow solutions on the triangular meshes. Because the use of quadrilateral-triangular meshes is better than that of purely triangular meshes in the study of steady flows,⁴ it is worthwhile to create a solution-adaptive approach for unsteady flow calculations on quadrilateral-triangular meshes.

In computation of unsteady flows, adaptive mesh techniques are generally divided into three categories: 1) mesh regeneration,² 2) mesh movement,⁵ and 3) mesh enrichment.^{1,3} Considering accuracy, efficiency, simplicity, and flexibility, the mesh enrichment method is adopted in this work. During the process of mesh enrichment, the following two problems should be addressed: 1) how the flow properties at the nodes and centers of new cells are calculated to obtain the spatially accurate values and 2) when the mesh is refined to achieve the time-accurate solutions. For the first problem, several weighted-averaging procedures¹ and scattered data interpolation approaches⁶ were introduced. In the present paper, a minimum norm network (MNN) method, that was formulated on triangular meshes by Nielson and Franke,⁶ is modified and applied to interpolate the new node and cell-centered values on quadrilateral-triangular meshes. For the second problem, in most previous works, such as Refs. 1 and 3, the mesh has been spatially adapted every constant time step during the calculations. If this kind of approach is used, the mesh system can not adjust itself simultaneously with the time-varying flow solutions. In other words, the mesh will lag the solution in time. To solve this problem, Bockelie and Eiseman⁵ presented a prediction-correction method for grid movement. The data transfer from the old grid to the new grid, however, introduced the numerical error due to the interpolation. Also, extra computer time was required to operate this prediction-correction method. Instead of using the foregoing two approaches, a simple method is presented in this paper. By using this method, the mesh can be properly adapted in time according to the unsteady flow solutions, and the numerical error due to interpolation and extra computer time⁵ will be reduced or avoided.

The purpose of this work is to develop a solution-adaptive approach for unsteady inviscid flow calculations on quadrilateral-

triangular meshes. This approach includes a locally implicit total variation diminishing (TVD) scheme⁴ and an adaptive mesh technique. To evaluate the present interpolation algorithm, sinusoidal, exponential, $(x+y)^2$ and $(x+y)$ functions are tested. Based on the numerical results for the shock propagation in a channel, the present solution-adaptive approach is accurate, reliable, and suitable for studying unsteady inviscid flows.

Euler Solution Procedure and Adaptive Mesh Technique

In this work, the two-dimensional unsteady Euler equations are solved in the X - Y Cartesian coordinate system. The locally implicit cell-centered finite volume TVD scheme that was formulated on the quadrilateral-triangular meshes by Hwang and Yang⁴ was employed. About the shock propagation in a channel, adiabatic and no-penetration conditions are imposed on the wall surface. The pressure values at the wall are extrapolated from those at the interior cells. The upstream flow condition is imposed, and the flow properties at the exit plane are extrapolated from those at the interior cells.

The present adaptive mesh technique includes an enrichment indicator $|\nabla\rho|$ (magnitude of density gradient), an unstructured mesh generation method,² a mesh enrichment method, and an interpolation algorithm. For the mesh enrichment method, a coarse mesh is used as a background grid, and a two-level refinement procedure is created. If the value of $|\nabla\rho|$ for any one of the unrefined cells on the current mesh during the unsteady calculations is larger than a threshold value, the mesh enrichment is operated on the background grid. After finishing the generation of an intermediate mesh, the properties at all added new nodes are interpolated from those at the background nodes. Similar to first-level mesh refinement, second-level refinement on the intermediate mesh is continued. After that, the new computational mesh is completed. The diagrams for possible mesh enrichment situations and the detailed description of the mesh enrichment procedure are given in Ref. 7. Because Webster et al.³ showed that the mesh coarsening accounted for the majority of the central processing unit (CPU) cost for each enrichment step, the mesh coarsening procedure is not used in this work. According to the preceding discussion, the CPU time due to mesh coarsening and the numerical error arising from the interpolation of flow properties at new nodes are avoided or reduced. Also, the mesh system can adjust itself with time-varying flow solutions. As for the interpolation algorithm, a minimum norm network method that was formulated on triangular meshes by Nielson and Franke⁶ is modified and applied to interpolate the new node and cell-centered values during the mesh enrichment on quadrilateral-triangular meshes. With respect to the slopes of flow properties at the nodes, the minmod functions are introduced to eliminate the numerical noise around the shock regions. The mathematical formula and detailed explanations are provided in Ref. 7.

Results and Discussion

To understand the characteristics of present interpolation algorithm, two kinds of triangular-quadrilateral meshes (see Fig. 1) are used to achieve the numerical interpolations for $\sin(x+y)$, $\exp(x+y)$, $(x+y)^2$, and $(x+y)$ functions. For each cell on those two meshes, the coordinates of the centroid and the exact values at related nodes are calculated first. Then the values of $\sin(x+y)$, $\exp(x+y)$, $(x+y)^2$, and $(x+y)$ at those centroids are obtained by using corresponding node values and the present interpolation algorithm. If the test function is linear, such as $(x+y)$, the interpolation errors for the Laplacian weighted-averaging method and present algorithm (see Table 1) are near the machine error (single precision). The accuracy of the Laplacian weighted-averaging method is better than the present algorithm. If the test functions are nonlinear, however, such as $\sin(x+y)$, $\exp(x+y)$, and $(x+y)^2$, the error analysis (see Table 1) indicates that the present algorithm is the best one among three methods. In the computations of unsteady inviscid flows, the Euler solutions are almost nonlinear. Therefore, the present interpolation algorithm is recommended.

To study the accuracy and efficiency of the present solution-adaptive approach on quadrilateral-triangular meshes, shock prop-

Received Sept. 24, 1994; revision received June 8, 1995; accepted for publication June 8, 1995; presented as Paper 95-1723 at the AIAA 12th Computational Fluid Dynamics Conference, San Diego, CA, June 19-22, 1995. Copyright © 1995 by the American Institute of Aeronautics and Astronautics, Inc. All rights reserved.

*Professor, Institute of Aeronautics and Astronautics, 1 University Road, Member AIAA.

†Graduate Student, Institute of Aeronautics and Astronautics, 1 University Road.

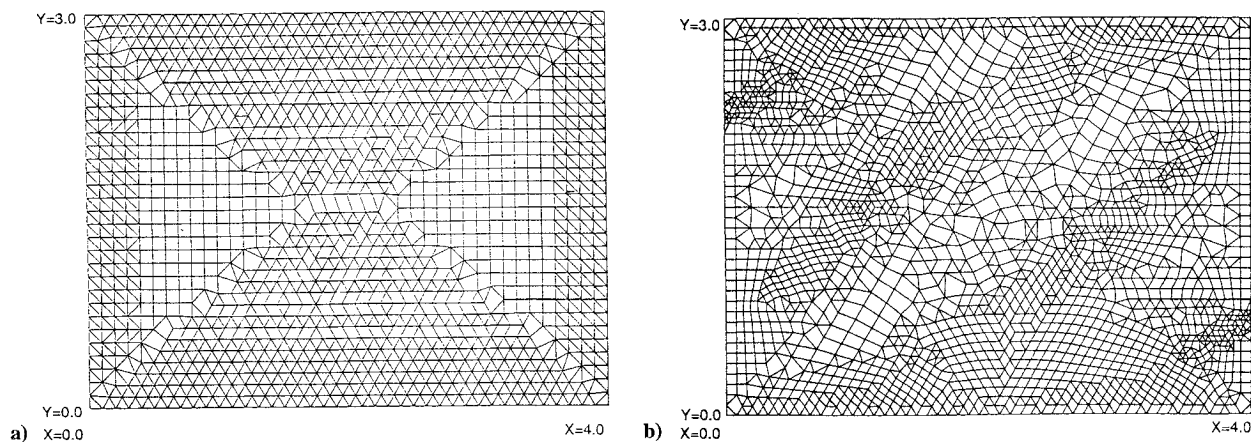


Fig. 1 Meshes for evaluation of the present interpolation algorithm for $\sin(x+y)$, $\exp(x+y)$, $(x+y)^2$, and $x+y$ functions: a) regular mesh, 1594 triangles and 472 quadrilaterals; and b) highly irregular mesh, 1114 triangles and 1496 quadrilaterals.

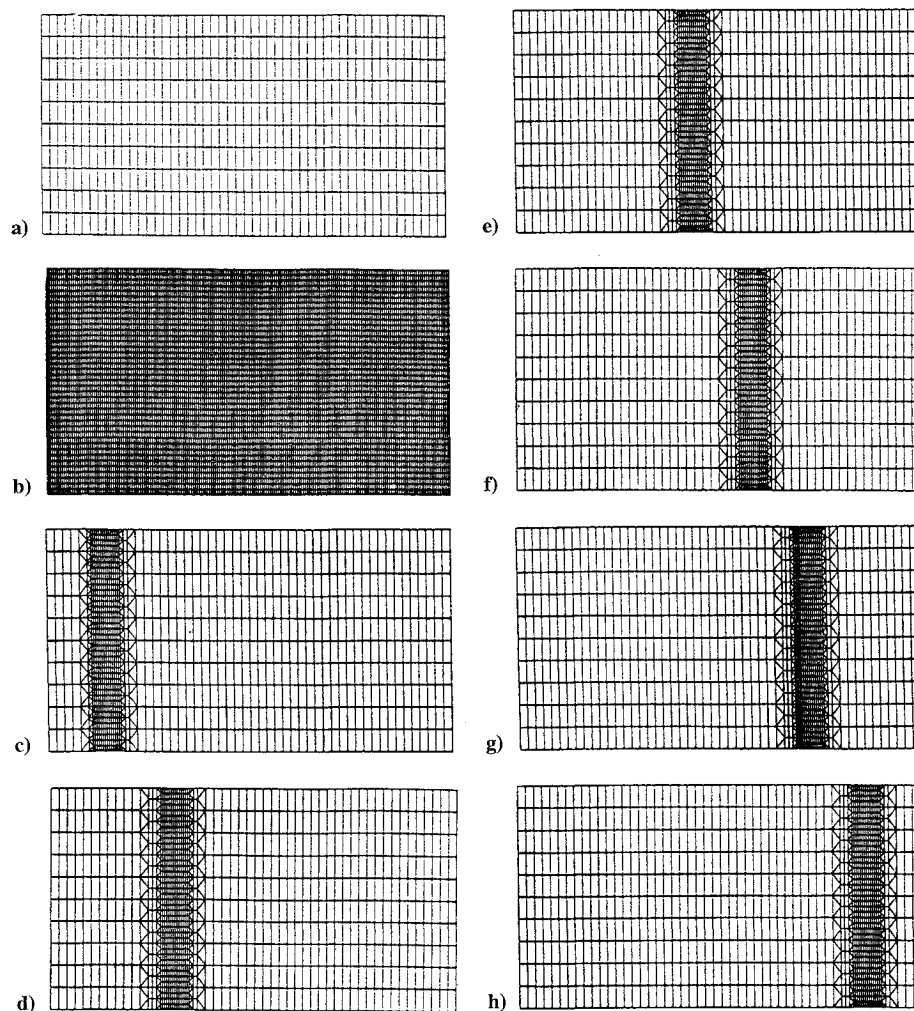


Fig. 2 Meshes for the shock propagation in a channel: a) coarse mesh, background grid, 500 elements; b) fine mesh, 8000 elements; c) $T = 0.1$, 1190 elements; d) $T = 0.2$, 1220 elements; e) $T = 0.3$, 1220 elements; f) $T = 0.4$, 1220 elements; g) $T = 0.5$, 1220 elements; and h) $T = 0.6$, 1220 elements.

agation in a channel is investigated. In this problem, the shock with a shock Mach number 1.4 moves to the right side of a channel from the position $X = 0.0$ at $T = 0.0$. The meshes and corresponding pressure distributions along the lower surface are shown in Figs. 2 and 3, respectively. During the calculation, a coarse mesh (see Fig. 2a) is used as the background grid. At the 10th time step, the coarse mesh is refined first. Later, the coarse mesh is automatically enriched by using the present solution-adaptive approach. The meshes at $T = 0.1, 0.2, 0.3, 0.4, 0.5$, and 0.6 are plotted in Figs. 2c–2h, and the average number of elements of those meshes is 1215. From those time-varying meshes and the corresponding pressure

distributions along the lower wall (see Fig. 3), the coarse mesh is automatically refined around the moving shock. If the coarse mesh is not enriched during the unsteady calculations, the pressure distributions along the lower wall indicate that the numerical overshoots appear after the shocks and increase with time. When a fine mesh (see Fig. 2b) is used and is not changed during the calculations, the aforementioned overshoots disappear, and the solutions are better than those on the coarse mesh. Comparing with the exact solutions, the pressure distributions on the present adaptive meshes are the best ones among those three kinds of computations (see Fig. 3). The computation on the adaptive meshes takes approximately 2.5

Table 1 Error analysis^{a,b} of present interpolation algorithm, Laplacian, and reciprocal distance weighted-averaging methods

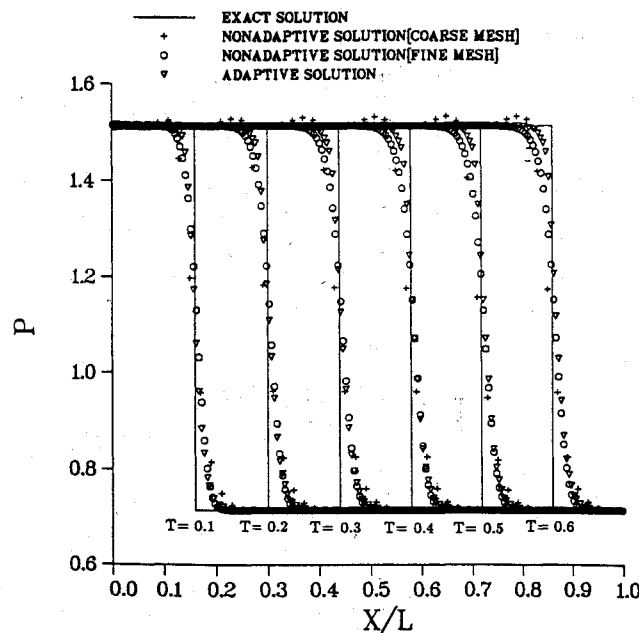
Method ^c	Mesh ^d	$\sin(x+y)$	$\exp(x+y)$	$(x+y)^2$	$(x+y)$
1	1	-3.67	-1.36	-3.15	-5.90
2	1	-2.86	-0.54	-2.40	-6.66
3	1	-2.16	0.40	-1.08	-1.99
1	2	-3.68	-1.22	-3.21	-6.05
2	2	-2.94	-0.61	-2.49	-6.66
3	2	-2.38	0.003	-1.35	-2.25

^aThe present error analysis is performed on VAX 8600.

^bThe values of interpolation error are calculated by the expression $\log_{10}(\sqrt{\sum_i \Delta_i^2}/Ne)$. In this mathematical expression, Ne indicates the number of cells and Δ_i represents the value of numerical difference between exact and interpolation results at centroid of cell i .

^cThe following three interpolation methods are used: 1) present interpolation algorithm, 2) Laplacian weighted-averaging method, and 3) reciprocal distance weighted-averaging method.

^dThe following two kinds of meshes are used: 1) Fig. 1a (1594 triangles and 472 quadrilaterals) and 2) Fig. 1b (1114 triangles and 1496 quadrilaterals).

**Fig. 3** Pressure distributions along the lower wall for the shock propagation in a channel.

times the CPU time required to run the flow solver on the coarse mesh. The CPU time required for the computation on the fine mesh, however, is about 3.5 times that required for the computation on the adaptive mesh. Based on the preceding discussion, the accuracy and efficiency of present solution-adaptive approach are confirmed.

Conclusions

To study the unsteady inviscid flow problems, a solution-adaptive approach has been presented in this paper. An adaptive mesh technique is developed on quadrilateral-triangular meshes and incorporated with the Euler solution procedure, that includes a locally implicit cell-centered finite volume TVD scheme⁴ and the numerical treatments of boundary conditions. For the present adaptive mesh technique, an unstructured mesh generation method² is adopted. The magnitude of density gradient $|\nabla \rho|$ is chosen as the enrichment indicator. To reduce the CPU time and numerical error arising from the mesh coarsening and the interpolation of flow properties, a two-level refinement technique and an interpolation algorithm are created. From the error analysis for $\sin(x+y)$, $\exp(x+y)$, $(x+y)^2$, and $(x+y)$ functions, the present interpolation algorithm is accurate. For the shock propagation in a channel, the meshes can be properly refined in time according to the unsteady flow solutions. On the coarse, fine, and adapted meshes, respectively, the pressure distributions along the lower wall and CPU time required for those computations indicate that the present solution-adaptive approach is accurate, efficient, and reliable.

References

- ¹Rausch, R. D., Batina, J. T., and Yang, H. T. Y., "Spatial Adaptation of Unstructured Meshes for Unsteady Aerodynamic Flow Computations," *AIAA Journal*, Vol. 30, No. 5, 1992, pp. 1243-1251.
- ²Hwang, C. J., and Wu, S. J., "Global and Local Remeshing Algorithms for Compressible Flows," *Journal of Computational Physics*, Vol. 102, No. 1, 1992, pp. 98-113.
- ³Webster, B. E., Shephard, M. S., Rusak, Z., and Flaherty, J. E., "Automated Adaptive Time-Discontinuous Finite Element Method for Unsteady Compressible Airfoil Aerodynamics," *AIAA Journal*, Vol. 32, No. 4, 1994, pp. 748-757.
- ⁴Hwang, C. J., and Yang, S. Y., "Locally Implicit Total Variation Diminishing Schemes on Mixed Quadrilateral-Triangular Meshes," *AIAA Journal*, Vol. 31, No. 11, 1993, pp. 2008-2015.
- ⁵Bockelie, M. J., and Eiseman, P. R., "A Time-Accurate Adaptive Grid Method and the Numerical Simulation of a Shock-Vortex Interaction," NASA TP-2998, March 1990.
- ⁶Nielson, G. M., and Franke, R., "Surface Construction Based Upon Triangulations," *Surfaces in CAGD*, edited by R. E. Barnhill and W. Boehm, North-Holland, Amsterdam, 1983, pp. 163-177.
- ⁷Hwang, C. J., and Fang, J. M., "Solution-Adaptive Approach for Unsteady Flow Calculations on Quadrilateral-Triangular Meshes," AIAA Paper 95-1723, June 1995.

Fluorescence Velocity Measurements in the Interior of a Hydrogen Arcjet Nozzle

P. Victor Storm* and Mark A. Cappelli†
Stanford University, Stanford, California 94305-3032

Introduction

As arcjet thrusters have advanced from laboratory devices to in-flight operational thrusters for satellite north-south station-keeping, there has been an increase in interest in improving arcjet efficiency and operating range. These improvements will be obtained primarily through advanced analytical modeling of arcjets; however, validation of the models can be performed only by comparison with experimental measurements of operating parameters and plasma properties. During the past several years, a number of optical diagnostics have been developed to investigate properties in the plasma plume of the arcjet. Primary among these diagnostics is laser-induced fluorescence (LIF), which has proven very useful because of its abundant signal level, very good spatial resolution, and specie-specific nature. Plasma properties in the plume of an arcjet thruster operating on a variety of propellants have been measured using LIF. Liebeskind et al.¹ measured atomic hydrogen translational temperature and velocity at the exit plane of a 1-kW hydrogen arcjet thruster, and investigated slip velocity by the fluorescence of helium in a helium-seeded hydrogen arcjet.² Ruyten and Keefer³ measured velocity in an argon plume of a 0.3-kW arcjet, and Ruyten et al.⁴ performed LIF on atomic hydrogen and nitrogen to measure velocity in a 1-kW arcjet plume using simulated ammonia as the propellant. Recently, Pobst et al.⁵ measured ground-state atomic hydrogen density, temperature, and velocity profiles at the exit plane of a 1-kW hydrogen arcjet using pulsed two-photon LIF.

Although LIF has been successfully applied to arcjet thrusters as a plasma plume diagnostic, it has not been used previously to investigate plasma properties within the nozzle because of geometric constraints and reduced signal-to-background noise ratios. Optical studies of the plasma in the interior of the arcjet were performed

Received Aug. 14, 1995; revision received Oct. 25, 1995; accepted for publication Nov. 14, 1995. Copyright © 1995 by the American Institute of Aeronautics and Astronautics, Inc. All rights reserved.

*Research Assistant, High Temperature Gasdynamics Laboratory, Department of Mechanical Engineering, Student Member AIAA.

†Associate Professor, High Temperature Gasdynamics Laboratory, Department of Mechanical Engineering, Member AIAA.